



Original Articles

Load applied on osseointegrated implant by transfemoral bone-anchored prostheses fitted with state-of-the-art prosthetic components

Laurent Frossard^{a,b,c,d,*}, Stefan Laux^e, Marta Geadá^e, Peter Paul Heym^f, Knut Lechler^g

^a YourResearchProject Pty Ltd, PO Box 143, Red Hill, QLD 4059, Australia

^b Griffith University, 1 Parklands Dr, Southport, QLD 4215, Australia

^c University of the Sunshine Coast, 90 Sippy Downs Dr, Sippy Downs, QLD 4556, Australia

^d Queensland University of Technology, 2 George St, Brisbane, City, QLD, 4000, Australia

^e APC Prosthetics Pty Ltd, Suite 1, 170-180 Bourke Rd, Alexandria, NSW 2015, Australia

^f Sum of Squares - Statistical Consulting, Essener Str. 100, 04357 Leipzig, Germany

^g ÖSSUR, R&D, Medical Office, Grjótals 1-5, Reykjavík, Iceland

ARTICLE INFO

Keywords:

Amputation
Artificial limbs
Bone-anchored prosthesis
Bionics
Kinetics
Loading
Prosthesis

ABSTRACT

Background: This study presented the load profile applied on transfemoral osseointegrated implants by bone-anchored prostheses fitted with state-of-the-art ÖSSUR microprocessor-controlled Rheo Knee XC and energy-storing-and-returning Pro-Flex XC or LP feet during five standardized daily activities.

Methods: This cross-sectional cohort study included 13 participants fitted with a press-fit transfemoral osseointegrated implant. Loading data were directly measured with the tri-axial transducer of an iPecsLab (RTC Electronics, USA) fitted between the implant and knee unit. The loading profile was characterized by spatio-temporal gait variables, magnitude of loading boundaries as well as onset and magnitude of loading extrema during walking, ascending and descending ramp and stairs.

Findings: A total of 2127 steps was analysed. The cadence ranged between 36 ± 7 and 47 ± 6 strides/min. The absolute maximum force and moments applied across all activities was 1322 N, 388 N and 133 N as well as 22 Nm, 52 Nm and 88 Nm on and around the long, anteroposterior and mediolateral axes of the implant, respectively.

Interpretation: This study provided new benchmark loading data applied by transfemoral bone-anchored prostheses fitted with selected ÖSSUR state-of-the-art components. Outcomes suggested that such prostheses can generate relevant loads at the interface with the osseointegrated implant to restore ambulation effectively. This study is a worthwhile contribution toward a systematic recording, analysis, and reporting of ecological prosthetic loading profiles as well as closing the evidence gaps between prescription and biomechanical benefits of state-of-the-art components. Hopefully, this will contribute to improve outcomes for growing number of individuals with limb loss opting for bionic solutions.

1. Introduction

Because the use of a prosthesis is essential to maintain quality of life of an individual with transfemoral amputation (TFA), providers of prosthetic care design, select and fit sockets, knees and feet components the most susceptible to maximize functional outcomes (Samuelsson et al., 2012). Unfortunately, the soft tissues of the residuum have limited capacity to withstand the mechanical constraints transmitted by the prosthesis through the socket during weight bearing. Practically, the interface between the residuum and the socket could generate

substantial discomfort due to skin breakdown that might lead to early, temporary and, possibly, definitive prosthesis abandonment (Meulenbelt et al., 2006).

Alternatively, TFAs could be fitted with bone-anchored prostheses (BAP) attached to an osseointegrated implant surgically inserted into the residual femur (Branemark et al., 2001; Pitkin, 2013). Several studies demonstrated that transfemoral BAP could improve functions and health-related quality of life, particularly for young and active individuals experiencing overwhelming socket issues (Atallah et al., 2020; Hagberg and Branemark, 2009; Hebert et al., 2017; Hoyt et al., 2020;

* Corresponding author at: YourResearchProject Pty Ltd, PO Box 143, Red Hill, QLD 4059, Australia.

E-mail address: laurentfrossard@outlook.com (L. Frossard).

<https://doi.org/10.1016/j.clinbiomech.2021.105457>

Received 30 June 2020; Accepted 17 August 2021

Available online 24 August 2021

0268-0033/© 2021 The Authors.

Published by Elsevier Ltd.

This is an open access article under the CC BY-NC-ND license

(<http://creativecommons.org/licenses/by-nc-nd/4.0/>).

Leijendekkers et al., 2017; van Eck and McGough, 2015). Management of residual soft tissues as well as risks of infections, loosening, periprosthetic fracture and breakage of osseointegrated implant parts are deemed acceptable by treating teams, although they are yet to be satisfactorily resolved (Atallah et al., 2018; Atallah et al., 2020; Hoyt et al., 2020; Kunutsor et al., 2018; van Eck and McGough, 2015). Preliminary health economic analyses suggested the cost-effectiveness of BAP compared to socket prostheses from a governmental prosthetic care perspective (Frossard et al., 2017; Frossard et al., 2018a; Frossard et al., 2018b; Frossard et al., 2019a).

2. Prescription of prosthetic components

Benefits and harms of the osseointegrated implants are confounded, one way or the other, by the fitting of prosthetic components during the rehabilitation and beyond (Helgason et al., 2009; Lee et al., 2008a; Newcombe et al., 2013; Stenlund et al., 2017; Stephenson and Seedhom, 2002; Thesleff et al., 2018). Clinical teams make bespoke recommendations for components considering altogether the regulation, type of implant, manufacturer's instructions, lifestyle and price tag (Morgenroth, 2013). Initially, mechanically passive components with basic functions like single-axis or polycentric hydraulic knees and multi-axial foot-ankle units were recommended (Lee et al., 2007; Lee et al., 2008b). Nowadays, the prescriptions of advanced components such as microprocessor-controlled knees (MPKs) and energy-storing-and-returning feet (ESARs) are more common (Frossard, 2013; Juhnke et al., 2015; Kaufman et al., 2012; Struchkov and Buckley, 2016). Prescription of these components is even considered as best-practice by some teams (OPRA, 2016).

3. Importance of loading profile

Frossard et al. (2003, 2008, 2011a) and Robinson et al. (2020a) highlighted that the biomechanical advantages of these components (e.g., increased functions, reduced exposure to adverse events) derive from the loading profile they generate, corresponding to the repeated pattern of the forces and moments applied on and round the three anatomical axes of osseointegrated implant during daily activities (Frossard et al., 2003; Frossard et al., 2008; Frossard et al., 2011a; Robinson et al., 2020a; Robinson et al., 2020b).

In principle, BAP fitted with MPKs and ESARs could increase stability (e.g., stance and swing control), walking capacity (e.g., high range of motion, mechanically-powered push off), attenuation of excessive loading during daily activities (e.g., auto adaptive stance and swing phases) and reduce risks of falls (e.g., automatic stumble recovery) (Campbell et al., 2020; Frossard, 2013; Highsmith et al., 2010; Kahle et al., 2008; Orendurff et al., 2006; Sawers and Hafner, 2013). One could hypothesise that these functions altogether might generate a loading profile within the Goldilocks Zone for the osseointegrated implant. As described in Pitkin and Frossard (2021) and further illustrated in the supplement, this concept of loading Goldilocks Zone refers to the zone where the mechanical constraints (e.g., magnitude of the forces and moments) applied on the implant and the residuum is within a range that is just right, not too low and not too high, to maintain the stability between the bone/implant coupling (Pitkin and Frossard, 2021). It is anticipated that the load applied by BAP fitted with state-of-the-art components might be likely to be in a safe zone (e.g., "suitable-loading" for stable osseointegration) rather than in more risky zones that could damage the bone/implant coupling (e.g., "under-loading" associated with early loosening and infection, "over-loading" leading to breakage of parts and periprosthetic fractures).

4. Current knowledge of loading profile

Unfortunately, this hypothesis could only be partially validated with the current understanding of loading profile applied by BAP estimated

using inverse dynamics or measured with a transducer (Dumas et al., 2009; Dumas et al., 2017; Frossard et al., 2011b; Harandi et al., 2020; Niswander et al., 2020; Thesleff et al., 2018).

Lee et al. (2007, 2008) reported some loading characteristics during walking, ascending and descending ramp and stairs for a cohort of TFAs fitted screw-type implants and basic components (e.g., mechanically passive knees, multi-axial foot-ankle) (Frossard, 2019; Lee et al., 2007; Lee et al., 2008b). Frossard et al. (2013) presented a single-case study showing that the characterization of the loading profile using a series of extrema has the capacity to differentiate BAP fitted with a mechanical and MPK knees (Frossard, 2013). Recently, Frossard et al. (2019b) completed, compiled and shared the data collected during these studies (Frossard, 2019).

5. Need for loading profile with state-of-the-art components

To date, evidence confirming the alleged biomechanical advantages of state-of-the-art components are sparse. Clearly, there is a need for a better understanding of loading profile applied by BAP fitted with state-of-the-art components during daily activities (Niswander et al., 2020).

Collecting new kinetic information on Rheo Knee XC and Pro-Flex XC or LP ankle-foot units (ÖSSUR, Iceland) will be indicated as they are amongst the MPKs and ESARs components commonly recommended to individuals with osseointegrated implant treated in Australia and elsewhere, respectively.

6. Purposes

The long-term aim of this work was to contribute to a better understanding of the mechanical effects of BAP fitted with state-of-the-art components on lower limb osseointegrated implants.

The purpose of this cross-sectional cohort study was to present the load profile applied on transfemoral osseointegrated implant by BAP fitted with Rheo Knee XC and Pro-Flex XC or LP using wearable transducer technology across five daily activities.

The specific objective was to present the range and variability of spatio-temporal gait variables, magnitude of loading boundaries as well as onset and magnitude of extrema applied during standardized straight level walking, ascending and descending ramp activities.

The supplement of this manuscript provides more information about the Goldilocks Zone, the position of transducer in relation to the implant, and the detection of extrema. Furthermore, eventual subsequent literature reviews and meta-analyses could be facilitated by additional information to be published in Data In Brief detailing the confounders (e.g., selection criteria, demographics, amputations data, prosthesis information, connections between implant and transducer, alignment of instrumented prostheses, position of percutaneous part and knee in relation to transducer, description of non-experimental setup, breakdown of number of steps analysed per activity), loading boundaries as well as scatter plots showing the dispersion of extrema detected and box plots of magnitude of extrema.

7. Methods

7.1. Population

Participants were recruited by a local prosthetist using arm-length recruitment strategy based on similar selection criteria presented previously (e.g., circa 6–8 cm clearance to fit transducer, completion of rehabilitation, capable to walk independently for 200 m) (Frossard et al., 2003; Frossard et al., 2010a; Lee et al., 2007; Lee et al., 2008b). No exclusion criteria were applied for gender, ethnicity, height or functional level. A total of 13 TFAs fitted with a non-FDA approved press-fit implant were assessed in Sydney, Australia between Sept 2017 and Aug 2018 (i.e., Integral leg prosthesis, Eska Orthopedics GmbH, Germany; Osseointegration Prosthetic Limb, Permedica SPA, Italy) (Atallah et al.,

2020). Each participant signed a written ethical consent form approved by research organization's human ethics committee (Human Research Ethics Committee Certificate No 1600000332, Queensland University of Technology, Brisbane, Australia).

7.2. Prosthesis

Participants were fitted with an instrumented prosthesis made of tube and/or offset connector, iPecsLab's transducer (RTC Electronics, USA), Rheo Knee XC, Pro-Flex XC or LP feet and their own footwear (Frossard et al., 2019b; Frossard et al., 2020; Koehler et al., 2014). We purposely choose the XC and LP models within the Pro-Flex family usually recommended for patients in Australia because of their ability to tolerate high impact level.

A qualified and experienced prosthetist achieved static alignment by positioning the knee joint centre approximately three centimetres posteriorly to the vertical line of the bodies' centre of mass using the L.A.S. A.R. Posture (Ottobock, Germany) (Blumentritt, 1997). The prosthetist made the dynamic alignment and resistance adjustment for knee and foot that suited participants' preferences (Blumentritt, 2017). Participants were used to walk with an MPK fitted in their usual limb, as detailed in the supplement. Thus, approximately 15-min acclimation time with instrumented prosthesis was deemed sufficient to warrant required confidence and safety (Schmalz et al., 2014).

7.3. Recording

The loads were measured directly using an iPecsLab including a tri-axial transducer fitted between the participant's offset adapter and knee unit (Frossard, 2013; Lee et al., 2007; Lee et al., 2008b). The transducer recorded forces and moments at 200 Hz that were sent wirelessly to laptop nearby. The coordinate system of the transducer was aligned so that its vertical axis was co-axial with the long (LG) axis of the implant and the other axes corresponded to the anatomical anteroposterior (AP) and mediolateral (ML) directions of the implant. Forces acting along the three axes of the transducer were denoted as FLG, FAP and FML where compression, anterior and lateral forces were positive, respectively. Moments about the three axes of the transducer were denoted as MLG, MAP and MML where external, lateral and anterior moments were positive, respectively. Studies indicated that forces and moments measured by iPecsLab transducer had an accuracy better than 1 N and 1 Nm, respectively (Frossard et al., 2019b; Frossard et al., 2020; Koehler et al., 2014). Here, we considered that the medullar and percutaneous parts of the implant as well as the tube and/or adaptor were one rigid part. However, the co-linearity of the long axes of the implant and the transducer depended on the offset adapter.

The loads were measured while participants performed up to five trials in five standardized daily activities consecutively including straight level walking (i.e., open walkway: 13 m) ascending and descending ramp (i.e., incline: 3.77 deg) and stairs (i.e., stairs height: 17 cm). Participants were instructed to perform each activity at a self-selected comfortable pace and to use the handrail if needed. However, participants were advised to use the step-over-step (e.g., normal reciprocal stepping pattern) rather than step-by-step (e.g., placement of both feet on the same step before the next step) technique while ascending and descending stairs as described by Reid et al. (2007), if possible (Reid et al., 2007).

The calibration of the transducer was achieved at the end of the recording session when the prosthesis was removed using post recording bench top measurements (i.e., zero-offset).

7.4. Processing

The raw forces and moments were imported and processed in a customized Matlab software program (The MathWorks Inc., USA) as detailed previously (Frossard, 2013; Frossard et al., 2003; Frossard et al.,

2010a; Lee et al., 2007; Lee et al., 2008b). The load data was extracted applying the following step-by-step a process:

- *Step 1: Calibration.* Raw data for each trial was offset according to the magnitude of the load recorded during calibration.
- *Step 2: Detection of relevant segment.* The first and the last two to three strides recorded for each trial were discarded to analyse steps taken at a steady pace, outside of gait initiation and termination, respectively.
- *Step 3: Determination of gait events.* The plot of FLG was used to detect manually individual heel contacts and toe-offs events within the relevant segment for each trial (Frossard et al., 2019b).
- *Step 4: Normalization.* Datasets were time-normalized from 0 to 100 throughout the gait cycle (GC) or support phases (SUP) to facilitate averaging of trials as well as reporting of events and extrema in percentage of GC (%GC) or SUP (%SUP), respectively. Forces and moments data were also expressed as percentage of bodyweight (% BW, %BWm).

7.5. Analysis

The characterization of loading profile involved up to 33 variables for each activity given a total of 201 variables across all activities, corresponding to a series of:

- *Three spatio-temporal variables* per activity including the cadence for a given trial as well as the duration of GC in seconds and the support phases in %GC (Frossard et al., 2010a). The cadence was determined based of the duration between two consecutive heel contacts of the prosthetic limb and, therefore, expressed in strides per minute (stride/min). The cadence of prosthetic limb did not always equate to the number of steps ascended or descended during stairs activities depending on step-over-step or step-by-step technique (Reid et al., 2007).
- *12 loading boundaries* per activity including the minimum and maximum of the three components of forces and moments expressed in %BW and %BWm across all gait cycles in relevant segment regardless of the onset, respectively.
- *36 overall loading boundaries* across all activities including the minimum, maximum and absolute maximum of the three components of forces and moments expressed in N and %BW as well as Nm and %BWm, respectively.
- *Up to 18 loading extrema* per activity including up to three extrema for each of the three components of force and moment (Frossard, 2013; Frossard et al., 2003; Frossard et al., 2009; Lee et al., 2007; Lee et al., 2008b). An extremum was defined as a point of inflection of the loading pattern occurring consistently over successive steps for a given activity for all participants. Time of occurrence or onset and magnitude of each extremum was detected semi-automatically by searching the minimum or maximum loading magnitude within a pre-set time window.

Datasets for spatio-temporal variables, loading boundaries and extrema were generated by collating altogether the GCs for all trials for each activity. Datasets for the overall loading boundaries were extracted for all GCs across all activities together. All datasets were described in this manuscript by the mean and one standard deviation. Box plots showing lower and higher limits of 95% confidence interval, mean and outliers of the magnitude of extrema of forces and moments are also presented in the supplement.

The variability of a dataset was determined using the percentage of variation ($PV = \text{absolute} [(\text{standard deviation}/\text{mean}) \times 100]$). Giving the inter and intra-variability of loading data reported previously, we considered that PV inferior or superior to 20% indicated a low and high variability, respectively (Frossard, 2013; Frossard, 2019; Frossard et al., 2010a; Lee et al., 2007; Lee et al., 2008b).

8. Results

8.1. Participants

A total of 13 TFAs fitted with a press-fit implant participated in this study (2 females, 11 males, 57 ± 14 years, 1.78 ± 0.08 m, 86.31 ± 18.03 kg, 25.921 ± 4.734 kg/m², 17 ± 19 years since amputation, 2 ± 2 years since osseointegration, 28.38 ± 5.69 cm residuum length or $63 \pm 11\%$ of sound thigh). Individual demographics, amputations and prosthetics information are detailed in the supplement. This cohort represented approximately 3.2% and 1.3% of the population of TFA fitted with BAP in Australia and worldwide, respectively.

A total of 2127 GCs was analysed including 347, 252, 268, 236 and 180 recorded during walking, ascending and descending ramp and stairs, respectively.

8.2. Spatio-temporal gait variables

The cadence and durations of GC are presented in Table 1. All 12 (80%) spatio-temporal variables showed a low variability during walking, ascending and descending ramp as well as ascending stairs. Only three (20%) spatio-temporal variables showed a high variability during descending stairs.

8.3. Loading profile

Participants used a range of combinations of tube and/or offset connectors between the percutaneous parts and the transducer (i.e., no tube and no adapter: 15%, a tube and an adapter: 8%, a tube and no adapter: 8%, no tube and an adapter: 69%). We estimated that the distal end of the percutaneous part and the centre of the knee were positioned 1.61 ± 1.36 cm, 0.75 ± 0.68 cm and 9.07 ± 2.32 cm as well as 1.08 ± 1.16 cm, -0.69 ± 0.73 cm and -8.10 ± 0.35 cm from the centre of the transducer on the AP, ML and LG axes, respectively.

An overview of the mean and standard deviation pattern of the load applied on implant during the support phase of walking, ascending and descending ramp and stairs are presented in Figs. 1, 2 and 3, respectively.

8.4. Loading boundaries

The average loading boundaries applied during each activity are presented in Table 2. All average minimum and maximum loads showed high variability except the five (17%) average maximum loads for FLG applied during all activities.

The overall minimum and maximum load applied across all activities, respectively, ranged between:

- -298 N and 1322 N or -28% BW and 161% BW on FLG,
- -358 N and 388 N or -31% BW and 34% BW on FAP,
- -56 N and 133 N or -7% BW and 16% BW on FML,
- -22 Nm and 20 Nm or -2% BWm and 2% BWm on MLG,
- -52 Nm and 24 Nm or -6% BWm and 3% BWm on MAP,
- -67 Nm and 88 Nm or -9% BWm and 11% BWm on MML.

Table 1

Mean and standard deviation of spatio-temporal variables including cadence, duration of gait cycle (GC) and support phase with state-of-the-art components during daily activities.

	Walking			Ascending ramp			Descending ramp			Ascending stairs			Descending stairs		
Cadence (Strides/min)	47 ± 6		L	45 ± 4		L	45 ± 6		L	38 ± 6		L	36 ± 7		H
Gait cycle (s)	1.34 ± 0.22		L	1.34 ± 0.18		L	1.37 ± 0.21		L	1.55 ± 0.24		L	1.72 ± 0.60		H
Support (%GC)	63 ± 4		L	64 ± 6		L	63 ± 6		L	52 ± 6		L	52 ± 11		H

%SUP: percentage of the support phase, %BW: Percentage of the bodyweight, H: High PV, L: Low PV.

8.5. Loading extrema

A total of 43 out of 90 potential extrema across all activities were actually extracted as they occurred consistently for all participants (i.e., FLG1, FAP1, FAP2, FML1, MLG1, MLG2, MAP1, MML1, MML2, MML3), including ten for level walking and ascending ramp as well as nine for descending ramp, eight for ascending stairs and six for descending stairs.

The onset and magnitude presented in Table 3 showed a high variability for 31 (72%) and 38 (88%) extrema, respectively.

9. Discussion

9.1. Key results

This study indicated that:

- The loading profiles were obtained for a cohort representing approximately 1.3% of the estimated population of TFA fitted with BAP worldwide.
- Cadence ranged between 36 ± 7 and 47 ± 6 strides/min when walking, ascending and descending ramp and stairs at self-selected speed.
- The absolute maximum load applied was 161% BW on FLG, 34% BW on FAP, 16% BW on FML, 2% BWm on MLG, 6% BWm on MAP and 11% BWm on MML.
- The loading profile applied during the five daily activities considered could be characterized by a series of 10 extrema (i.e., FLG = 1, FAP = 2, FML = 1, MLG = 2, MAP = 1, MML = 3).
- The variability was typically low for the spatio-temporal variables but high for the loading boundaries and extrema.

9.2. Interpretation

Incidentally, this study confirmed the ability of portable kinetic systems using a tri-axial transducer embedded in the prosthesis to capture more ecological loading profile than other methods relying on inverse dynamics (Dumas et al., 2009; Dumas et al., 2017; Frossard et al., 2008; Frossard et al., 2010a; Frossard et al., 2010b; Frossard et al., 2011b; Lee et al., 2007; Lee et al., 2008b). Direct measurements allowed recording of high number of steps when the participants moved freely in a non-instrumented environment. These measurements alleviate some of the burdens of inverse dynamics requiring steps adjustments to hit the faceplates and positioning of reflective markers on the body to facilitate 3D motion capture. Inverse dynamic is also prone to propagation of error measurements to proximal joints as suggested in Dumas et al. (2017) (Dumas et al., 2009; Dumas et al., 2017; Frossard et al., 2011b). Thus, load profile measured directly with a transducer might be more reflective of real-world loading.

The comparison of the loading profile presented here with data previously published must be considered carefully because of possible differences between studies due to uncontrolled confounders (e.g., length of residuum, heterogeneity of prosthetic components, alignment due to inter-prosthetist variability, physical set-ups of the activities and duration of acclimation with instrumented prosthesis) (Frossard, 2019; Frossard et al., 2010a; Lee et al., 2007; Lee et al., 2008b). Nonetheless, this study indicated that BAP fitted with the state-of-the-art components

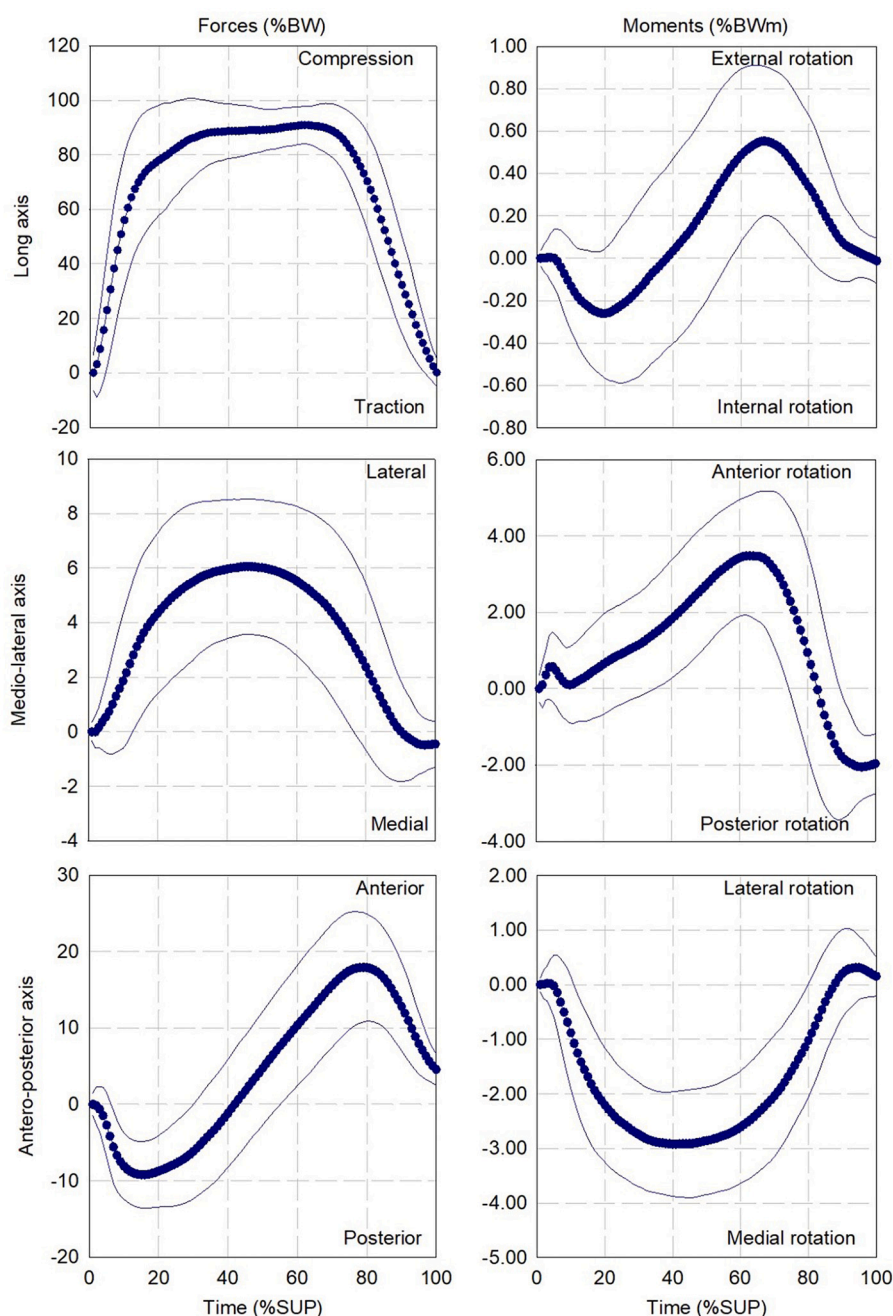


Fig. 1. Average and standard deviation (thin lines) of loading profile applied with state-of-the-art components during walking (347 gait cycles). %BW: Percentage of the bodyweight.

restore noticeably the spatio-temporal gait characteristics when ambulating at self-selected speed. The average cadence and durations of support phase during walking were 3 strides/min (5%) faster and 0.022 s (3%) longer, 0 strides/min and 0.112 s (13%) longer but 11 strides/min (24%) slower and 0.192 s (23%) longer compared to baseline for individuals fitted with socket-suspended prostheses and BAP including basic components as well as able-bodied presented in Frossard et al., 2010b, Frossard et al., 2019a, respectively (Frossard, 2019; Frossard et al., 2010a). State-of-the-art components produced maximum load across all the activities that was increased noticeably by 226 N or 37% BW on FLG but moderately by 77 N or 2% BW on FAP, 6 Nm or 1% BWm on MLG, 3 Nm or 2% BWm on MAP and 14 Nm or 3% BWm on MML and even reduced by 149 N or 11% BW on FML compared to BAP fitted with basic components (Frossard, 2019). State-of-the-art components

generated propelling loads during the last part of the support phase that were increased by 7% BW, 8% BW and 7% BW for FAP2, 2.61% BWm, 1.80% BWm and 0.89% BWm for MML2 as well as 0.29% BWm, 0.06% BWm and 0.31% BWm for MLG2 compared to BAP fitted with basic components during walking as well as ascending and descending ramp, respectively (Frossard, 2019).

Finally, the high variability in magnitude of extrema was consistent with step-to-step variabilities reported in Lee et al. (2008a) that are typical of symptomatic populations. There is little evidence associating high variability and exposure to risks for the implant. However, these outcomes underlined the benefits of individualized assessments when looking at effects of specific components on loading profile. They also highlighted the importance of considering components with homogeneous design when planning observational cohort studies.

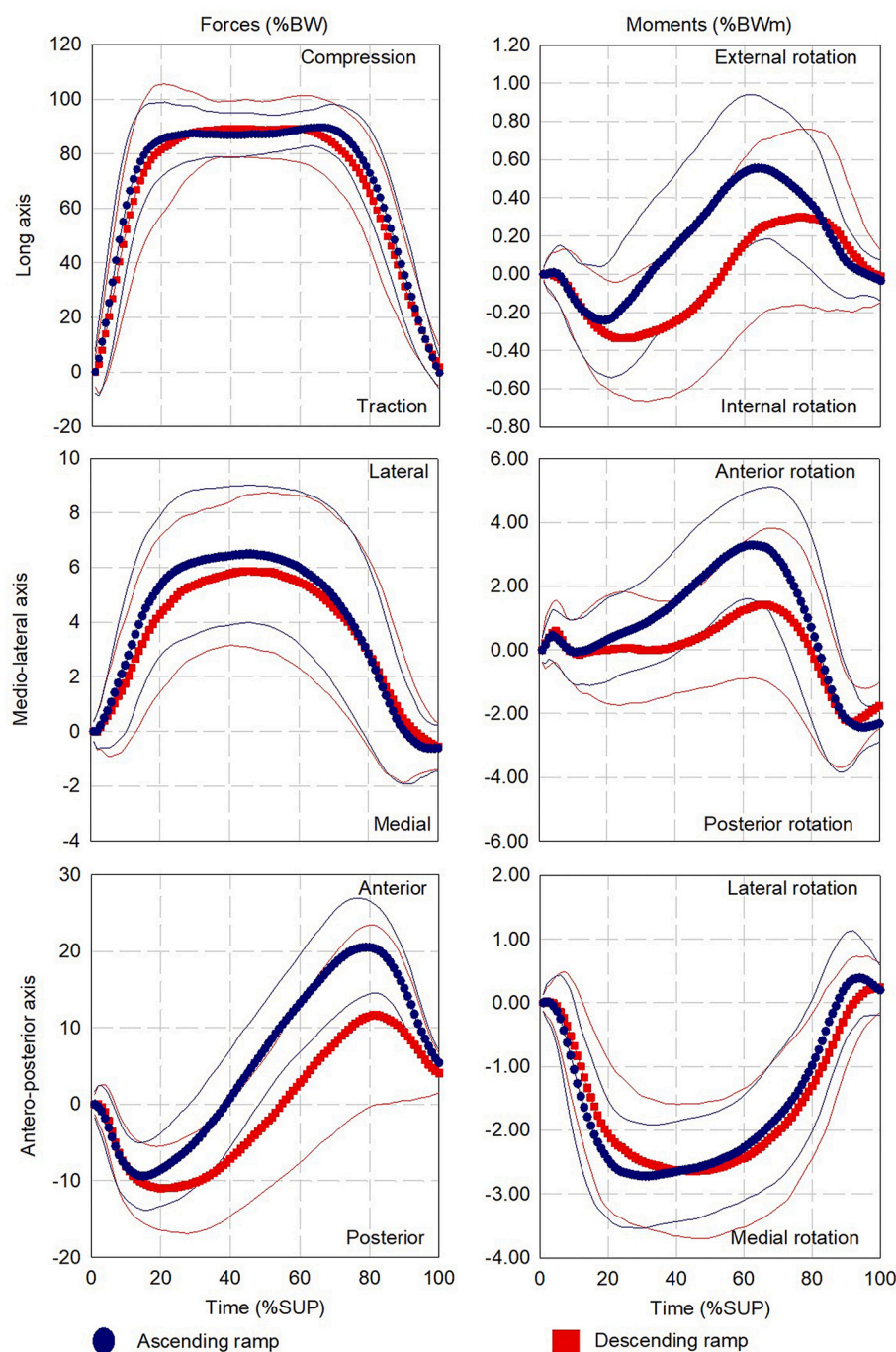


Fig. 2. Average and standard deviation (thin lines) of loading profile applied with state-of-the-art components during ascending (252 gait cycles) and descending ramp (268 gait cycles). %BW: Percentage of the bodyweight.

9.3. Limitations

The limitations of this work were typical of observational and, more specifically, cross-sectional cohort studies focusing on ecological measurements of prosthetic loading during standardized daily activities (Frossard et al., 2008; Frossard et al., 2010a; Lee et al., 2007; Lee et al., 2008b).

The forces and the moments were expressed in relation to the transducer's coordinate system. However, the transducer was offset by a few centimetres only on the AP and ML axes making the magnitude of the moments around these axes fairly close to the ones applied at the distal end of the implant. The measurements of the loads were performed without standardization of the resistance of knee flexion and

stiffness of the ankle units (e.g., index of anthropomorphicity) during dynamic alignments (Blumentritt, 2017; Frossard et al., 2019b; Kobayashi et al., 2013; Schmalz et al., 2002). It is unclear how individual adjustments affected the overall variability of loading profiles. Studies showed that the acclimation time allowed should be sufficient, giving prior experience of the participants with MKPs (Schmalz et al., 2014). However, it is possible that limited adaptation to various default stance and swing setups between knees might lead the more hesitant gait pattern and possibly lower loading. Prolonged practice would have helped participants to take full advantage of Rheo Knee XC's stair assist functions and, possibly, reduce variability of extrema particularly during descending stairs.

The characterization of the loading profile overlooked the loading

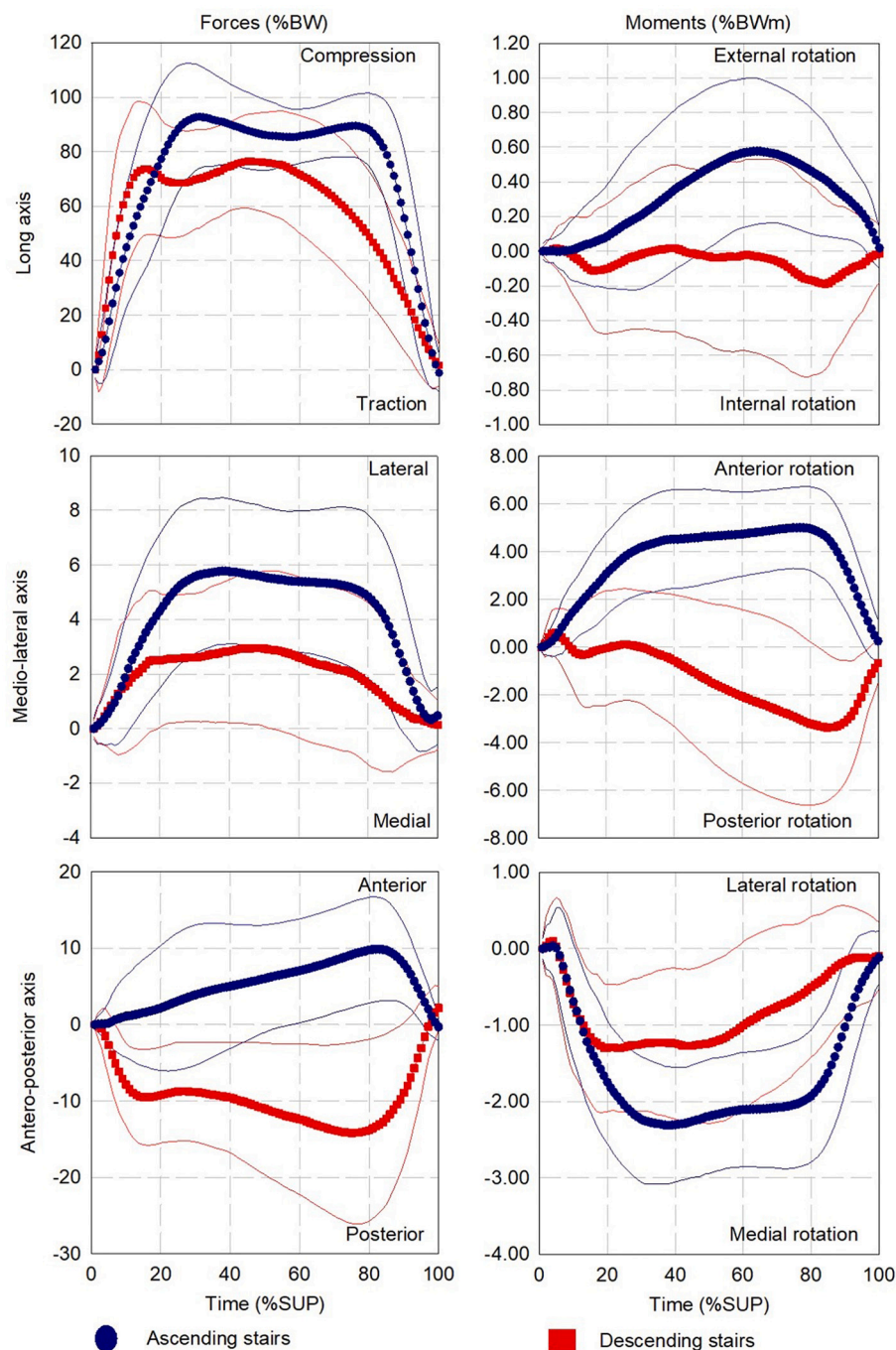


Fig. 3. Average and standard deviation (thin lines) of loading profile applied with state-of-the-art components during ascending (236 gait cycles) and descending stairs (180 gait cycles). %BW: Percentage of the bodyweight.

rate occurring during the first part of the support phase and the impulse applied during the whole GC. We made an educated choice for the interpretation of the PV's threshold.

The interpretation of the loading characteristics might be limited by the lack of assessment of confounders associated with spatial variables (e.g., walking base, step and stride length), as well as dynamics (e.g., ground and handrail reaction forces), kinematics (e.g., trunk bending, hip range of movement) and kinetics (e.g., ankle, knee, and hip joint moments and work). Unfortunately, the execution of the activities was too little documented to explain interactions between loading profiles and the execution of the activity, such as use of yielding function of the knee, positioning of feet and use of handrail during descending of the stairs. The Stair Assessment Index could have been one way to document

the execution of stair activities and should be considered in future studies (Kahle et al., 2008).

9.4. Generalization

This study provided new benchmark kinetic data for commonly prescribed state-of-the-art components fitted to transfemoral BAP. Comparable to most studies in the field, this sample size could be somewhat representative of current existing population. More importantly, this study relied on the analysis of a number of GCs that was larger than most studies relying on inverse dynamics, for example (Dumas et al., 2017; Frossard et al., 2011b). However, generalization of loading profiles might be considered carefully because of the high

Table 2

Loading boundaries of the magnitude of forces (F) and moments (M) on the long (LG), anteroposterior (AP) and mediolateral (ML) axes of osseointegrated implant applied by state-of-the-art components during daily activities.

	Walking		Ascending ramp		Descending ramp		Ascending stairs		Descending stairs	
Minimum										
FLG (%BW)	-3.81 ± 4.35	H	-4.12 ± 4.39	H	-2.01 ± 5.46	H	-3.40 ± 4.77	H	-2.39 ± 5.98	H
FAP (%BW)	-11.35 ± 4.19	H	-10.92 ± 4.05	H	-13.77 ± 5.80	H	-3.74 ± 5.37	H	-19.04 ± 8.53	H
FML (%BW)	-1.20 ± 0.80	H	-1.20 ± 0.82	H	-1.26 ± 1.10	H	-0.69 ± 0.70	H	-1.58 ± 1.68	H
MLG (%BWm)	-0.441 ± 0.283	H	-0.396 ± 0.239	H	-0.548 ± 0.278	H	-0.205 ± 0.182	H	-0.559 ± 0.410	H
MAP (%BWm)	-3.438 ± 0.982	H	-3.168 ± 0.832	H	-3.150 ± 1.065	H	-2.780 ± 0.802	H	-2.040 ± 0.811	H
MML (%BWm)	-2.469 ± 1.012	H	-2.922 ± 0.788	H	-2.833 ± 1.254	H	-0.346 ± 0.410	H	-4.315 ± 2.333	H
Maximum										
FLG (%BW)	101.97 ± 6.76	L	100.55 ± 6.88	L	105.43 ± 11.28	L	108.27 ± 9.56	L	95.48 ± 18.31	L
FAP (%BW)	19.74 ± 7.04	H	22.43 ± 6.00	H	15.72 ± 8.31	H	11.05 ± 6.33	H	3.60 ± 2.09	H
FML (%BW)	7.02 ± 2.72	H	7.62 ± 2.73	H	6.97 ± 3.06	H	6.96 ± 3.07	H	4.37 ± 2.35	H
MLG (%BWm)	0.734 ± 0.331	H	0.730 ± 0.358	H	0.603 ± 0.423	H	0.744 ± 0.387	H	0.426 ± 0.375	H
MAP (%BWm)	0.787 ± 0.523	H	0.821 ± 0.575	H	0.653 ± 0.492	H	0.486 ± 0.383	H	0.675 ± 0.534	H
MML (%BWm)	4.131 ± 1.208	H	4.027 ± 1.328	H	2.671 ± 1.570	H	5.701 ± 1.808	H	1.910 ± 1.502	H

%BW: Percentage of the bodyweight, H: High PV, L: Low PV.

Table 3

Mean and standard deviation of onset and magnitude of loading extrema of forces (F) and moments (M) on the long (LG) anteroposterior (AP) and mediolateral (ML) axes of osseointegrated implant applied by state-of-the-art components during daily activities.

	Walking		Ascending ramp		Descending ramp		Ascending stairs		Descending stairs	
Onset										
FLG1 (%SUP)	37.45 ± 18.32	H	37.85 ± 20.24	H	33.42 ± 15.48	H	36.60 ± 18.58	H	32.79 ± 21.46	H
FAP1 (%SUP)	18.03 ± 9.64	H	14.49 ± 6.51	H	22.54 ± 11.82	H	8.60 ± 9.76	H	53.06 ± 29.38	H
FAP2 (%SUP)	79.61 ± 6.20	L	79.87 ± 6.32	L	83.45 ± 8.17	L	81.66 ± 11.68	L	-	-
FML1 (%SUP)	43.31 ± 15.33	H	42.75 ± 16.87	H	45.39 ± 18.06	H	42.20 ± 19.95	H	39.84 ± 21.58	H
MLG1 (%SUP)	22.65 ± 13.20	H	19.21 ± 11.03	H	30.56 ± 15.84	H	16.35 ± 16.52	H	56.23 ± 31.08	H
MLG2 (%SUP)	67.07 ± 10.83	L	66.29 ± 11.19	L	72.96 ± 18.64	H	64.28 ± 18.73	H	-	-
MAP1 (%SUP)	36.11 ± 13.74	H	33.18 ± 13.27	H	41.96 ± 16.58	H	45.26 ± 19.79	H	36.21 ± 20.26	H
MML1 (%SUP)	9.00 ± 8.20	H	10.67 ± 8.75	H	59.95 ± 17.36	H	65.75 ± 19.79	H	83.49 ± 15.31	L
MML2 (%SUP)	65.79 ± 8.07	L	65.37 ± 8.02	L	89.03 ± 6.07	L	-	-	-	-
MML3 (%SUP)	89.14 ± 6.39	L	88.82 ± 6.27	L	-	-	-	-	-	-
Magnitude										
FLG1 (%BW)	101.97 ± 6.76	L	100.55 ± 6.88	L	105.33 ± 11.40	L	108.24 ± 9.57	L	95.48 ± 18.31	L
FAP1 (%BW)	-11.35 ± 4.19	H	-10.92 ± 4.05	H	-13.73 ± 5.77	H	-3.25 ± 5.60	H	-19.04 ± 8.53	H
FAP2 (%BW)	19.74 ± 7.04	H	22.43 ± 6.00	H	15.50 ± 8.74	H	11.01 ± 6.37	H	-	-
FML1 (%BW)	7.02 ± 2.72	H	7.61 ± 2.74	H	6.97 ± 3.06	H	6.95 ± 3.09	H	4.28 ± 2.46	H
MLG1 (%BWm)	-0.431 ± 0.291	H	-0.384 ± 0.247	H	-0.541 ± 0.283	H	-0.185 ± 0.192	H	-0.559 ± 0.410	H
MLG2 (%BWm)	0.734 ± 0.331	H	0.730 ± 0.358	H	0.598 ± 0.430	H	0.744 ± 0.388	H	-	-
MAP1 (%BWm)	-3.438 ± 0.982	H	-3.168 ± 0.832	H	-3.150 ± 1.065	H	-2.779 ± 0.802	H	-2.036 ± 0.814	H
MML1 (%BWm)	-0.751 ± 0.683	H	-0.865 ± 0.733	H	2.287 ± 1.974	H	5.696 ± 1.808	H	-4.307 ± 2.347	H
MML2 (%BWm)	4.096 ± 1.254	H	3.980 ± 1.381	H	-2.813 ± 1.234	H	-	-	-	-
MML3 (%BWm)	-2.466 ± 1.013	H	-2.920 ± 0.790	H	-	-	-	-	-	-

%SUP: percentage of the support phase, %BW: Percentage of the bodyweight, H: High PV, L: Low PV.

variability in extrema highlighting the importance of individual skills with the knee and, certainly, limited to the use of the Rheo Knee XC and Pro-Flex XC or LP feet considered here. Further generalization might be hazardous when considering other MPKs and ESARs giving specificity in design features of each component.

More generalizable is the methodological contribution toward a systematic recording, analysis and reporting of ecological prosthetic loading profiles during standardized daily activities. The proposed loading characterization could be used to support further evidence-based prescription of components for BAP.

9.5. Future studies

It will belong to future studies to establish to what extent BAP with the state-of-the-art components make ambulation less physically demanding and allow users to be active for longer bouts of activities (e.g., BAP fitted with state-of-the-art components Vs. BAP fitted with basic components) (Frossard et al., 2011a; Jarvis et al., 2017).

In the meantime, the proposed characterization of loading profile could facilitate future observational studies with larger cohorts of TFAs

comparing BAP constructs with other MPKs and ESARs (Hobara et al., 2020; Kannenberg et al., 2013; Kaufman et al., 2012; Lura et al., 2015; Morgenroth et al., 2018; Struchkov and Buckley, 2016). Indeed, the magnitude of loading boundaries and extrema presented here can help to determine the sample size of cohorts that are required for sufficient statistical power of a study. Subsequent observational studies will provide a better understanding of cross-correlation between loading and confounders (e.g., demographics, amputations information, spatio-temporal gait variables) as well as inter-component loading variability.

Further studies could associate the loading profiles with complementary mechanical (e.g., dynamics, kinematics, kinetics characteristics), physiological (e.g., electromyography of residuum muscles, metabolic energy consumption) and participant's experience (e.g., comfort score) information (Butowicz et al., 2020; Dumas et al., 2009; Dumas et al., 2017; Frossard et al., 2011b; Kaufman et al., 2018; Pantall et al., 2011). Establishing how prosthetic loading with state-of-the-art components influence the development of osseointegration around the implant and overall stability will be particularly valuable (e.g., modeling) (Helgason et al., 2009; Lee et al., 2008a; Newcombe et al., 2013; Prochor et al., 2020; Robinson et al., 2020a; Schwarze et al., 2014).

10. Conclusions

The spatio-temporal gait variables and magnitude of the propelling loads suggested that bone-anchored prostheses fitted with the state-of-the-art components considered can contribute to restore noticeably the capacity of individuals with transfemoral osseointegrated implant to ambulate. Despite the possible effects of confounders, this study provided early indication that loading profile applied by state-of-the-art components could stacked up favourably against basic components.

This work supported broader efforts made by biomechanists, engineers and clinicians to design quality insurance norms for osseointegrated implants, surgical procedures, rehabilitation and prosthetic fitting protocols with BAP.

Altogether, this study is a worthwhile contribution toward closing the evidence gaps between the current prescription and prosthetic care benefits of state-of-the-art components that will, hopefully, warrant upmost favourable outcomes for growing number of individuals with limb loss opting for bionic solutions worldwide.

Abbreviations

%BW	Percentage of bodyweight
%GC	Percentage of gait cycle
%SUP	Percentage of support phases
AP	Anteroposterior axis
BAP	Bone-anchored prosthesis
BW	Bodyweight
ESAR	Energy-storing-and-returning foot
F	Force
GC	Gait cycle
LG	Long axis
M	Moment
ML	Mediolateral axis
MPK	Microprocessor-controlled knee
N	Number of gait cycles
PV	Percentage of variation
SUP	Support phases of gait cycle
TFA	Individual with transfemoral amputation

Funding

This study was solely funded by ÖSSUR, Iceland. ÖSSUR has had no influence upon the design, data collection, analysis, or interpretation of this research study and no involvement in the decision to publish these results.

Declaration of Competing Interest

L. Frossard received compensations for the writing of the manuscript.
S. Laux has no conflict of interest.
M. Geada has no conflict of interest.
P. Heym received compensations for statistical analysis.
K. Lechler is employed by ÖSSUR that provided the state-of-the-art components.

Acknowledgments

The authors wish to acknowledge Kristleifur Kristjansson, Magnús Oddsson and Thor Fridriksson from ÖSSUR, Iceland for the development of this project as well as Scott Elliot, Kris Carroll and Cathy Howells from ÖSSUR, Australia and Miriam Grant from APC Prosthetics Pty Ltd. for their valuable contribution to organization of the data collection.

Appendix A. Supplementary data

Supplementary data to this article can be found online at <https://doi.org/10.1016/j.clinbiomech.2021.105457>.

References

- Atallah, R., et al., 2018. Complications of bone-anchored prostheses for individuals with an extremity amputation: a systematic review. *PLoS One* 13 (8), e0201821. <https://doi.org/10.1371/journal.pone.0201821>.
- Atallah, R., et al., 2020. Safety, prosthesis wearing time and health-related quality of life of lower extremity bone-anchored prostheses using a press-fit titanium osseointegration implant: a prospective one-year follow-up cohort study. *PLoS One* 15 (3), e0230027. <https://doi.org/10.1371/journal.pone.0230027>.
- Blumentritt, S., 1997. A new biomechanical method for determination of static prosthetic alignment. *Prosthetics Orthot. Int.* 21 (2), 107–113. <https://doi.org/10.3109/03093649709164538>.
- Blumentritt, S., 2017. Function of prosthesis components in lower limb amputees with bone-anchored percutaneous implants-Biomechanical aspects. *Unfallchirurg* 1–10. <https://doi.org/10.1007/s00113-017-0334-1>.
- Branemark, R., et al., 2001. Osseointegration in skeletal reconstruction and rehabilitation: a review. *J. Rehabil. Res. Dev.* 38 (2), 175–181.
- Butowicz, C.M., et al., 2020. Relationships between mediolateral trunk-pelvic motion, hip strength, and knee joint moments during gait among persons with lower limb amputation. *Clin. Biomech.* 71, 160–166. <https://doi.org/10.1016/j.clinbiomech.2019.11.009>.
- Campbell, J.H., Stevens, P.M., Wurdeman, S.R., 2020. OASIS 1: retrospective analysis of four different microprocessor knee types. *J. Rehab. Assist. Technol. Eng.* 7 <https://doi.org/10.1177/2055668320968476>, 2055668320968476.
- Dumas, R., Cheze, L., Frossard, L., 2009. Loading applied on prosthetic knee of transfemoral amputee: comparison of inverse dynamics and direct measurements. *Gait Posture* 30 (4), 560–562. <https://doi.org/10.1016/j.gaitpost.2009.07.126>.
- Dumas, R., Branemark, R., Frossard, L., 2017. Gait analysis of transfemoral amputees: errors in inverse dynamics are substantial and depend on prosthetic design. *IEEE Trans. Neural. Syst. Rehabil. Eng.* 25 (6), 679–685. <https://doi.org/10.1109/TNSRE.2016.2601378>.
- Frossard, L., et al., 2013. Load applied on a bone-anchored transfemoral prosthesis: characterisation of prosthetic components – A case study. *J. Rehabil. Res. Dev.* 50 (5), 619–634. <https://doi.org/10.1682/JRRD.2012.04.0062>.
- Frossard, L., 2019. Loading characteristics data applied on osseointegrated implant by transfemoral bone-anchored prostheses fitted with basic components during daily activities. *Data Brief* 26, 104492. <https://doi.org/10.1016/j.dib.2019.104492>.
- Frossard, L., et al., 2003. Development and preliminary testing of a device for the direct measurement of forces and moments in the prosthetic limb of transfemoral amputees during activities of daily living. *JPO: J. Prosthet. Orthot.* 15 (4), 135–142.
- Frossard, L., et al., 2008. Monitoring of the load regime applied on the osseointegrated fixation of a trans-femoral amputee: a tool for evidence-based practice. *Prosthetics Orthot. Int.* 32 (1), 68–78. <https://doi.org/10.1080/03093640701676319>.
- Frossard, L., et al., 2009. Load-relief of walking aids on osseointegrated fixation: instrument for evidence-based practice. *IEEE Trans. Neural. Syst. Rehabil. Eng.* 17 (1), 9–14. <https://doi.org/10.1109/TNSRE.2008.2010478>.
- Frossard, L., et al., 2010a. Functional outcome of Transfemoral amputees fitted with an Osseointegrated fixation: temporal gait characteristics. *JPO: J. Prosthet. Orthot.* 22 (1), 11–20. <https://doi.org/10.1097/JPO.0b013e3181ccc53d>.
- Frossard, L., et al., 2010b. Apparatus for monitoring load bearing rehabilitation exercises of a transfemoral amputee fitted with an osseointegrated fixation: a proof-of-concept study. *Gait Posture* 31 (2), 223–228. <https://doi.org/10.1016/j.gaitpost.2009.10.010>.
- Frossard, L., et al., 2011a. Categorization of activities of daily living of lower limb amputees during short-term use of a portable kinetic recording system: a preliminary study. *JPO: J. Prosthet. Orthot.* 23 (1), 2–11. <https://doi.org/10.1097/JPO.0b013e318207914c>.
- Frossard, L., Cheze, L., Dumas, R., 2011b. Dynamic input to determine hip joint moments, power and work on the prosthetic limb of transfemoral amputees: ground reaction vs knee reaction. *Prosthetics Orthot. Int.* 35 (2), 140–149. <https://doi.org/10.1177/0309364611409002>.
- Frossard, L., et al., 2017. Cost comparison of socket-suspended and bone-anchored Transfemoral prostheses. *JPO: J. Prosthet. Orthot.* 29 (4), 150–160. <https://doi.org/10.1097/jpo.0000000000000142>.
- Frossard, L., et al., 2018a. Development of a government continuous quality improvement procedure for assessing the provision of bone anchored limb prosthesis: a process re-design descriptive study. *Canad. Prosthet. Orthot. J.* 1 (2), 1–14.
- Frossard, L., Ferrada, L., Quincey, T., et al., 2021. Cost-Effectiveness of Transtibial Bone-Anchored Prostheses Using Osseointegrated Fixation: From Challenges to Preliminary Data. *JPO Journal of Prosthetics and Orthotics* 33, 184–195. <https://doi.org/10.1097/jpo.0000000000000372>.
- Frossard, L., Leech, B., Pitkin, M., 2019b. Automated characterization of anthropomorphic of prosthetic feet fitted to bone-anchored transtibial prosthesis. *IEEE Trans. Biomed. Eng.* 66 (12), 3402–3410. <https://doi.org/10.1109/TBME.2019.2904713>.
- Frossard, L., Leech, B., Pitkin, M., 2020. Loading applied on osseointegrated implant by transtibial bone-anchored prostheses during daily activities: preliminary characterization of prosthetic feet. *JPO: J. Prosthet. Orthot.* <https://doi.org/10.1097/jpo.0000000000000280>. Online First.
- Frossard, L.A., et al., 2018b. Cost-effectiveness of bone-anchored prostheses using osseointegrated fixation: myth or reality? *Prosthetics Orthot. Int.* 42 (3), 318–327. <https://doi.org/10.1177/0309364617740239>.

- Hagberg, K., Branemark, R., 2009. One hundred patients treated with osseointegrated transfemoral amputation prostheses: rehabilitation perspective. *J. Rehabil. Res. Dev.* 46 (3), 331–344.
- Harandi, V.J., et al., 2020. Individual muscle contributions to hip joint-contact forces during walking in unilateral transfemoral amputees with osseointegrated prostheses. *Comput Methods Biomech Biomed Engin* 1–11. <https://doi.org/10.1080/10255842.2020.1786686>.
- Hebert, J.S., Rehani, M., Stiegelmar, R., 2017. Osseointegration for lower-limb amputation: a systematic review of clinical outcomes. *JBJS Rev.* 5 (10), e10 <https://doi.org/10.2106/JBJS.RVW.17.00037>.
- Helgason, B., et al., 2009. Risk of failure during gait for direct skeletal attachment of a femoral prosthesis: a finite element study. *Med. Eng. Phys.* 31 (5), 595–600. <https://doi.org/10.1016/j.medengphy.2008.11.015>.
- Highsmith, M.J., et al., 2010. Safety, energy efficiency, and cost efficacy of the C-leg for transfemoral amputees: a review of the literature. *Prosthetics Orthot. Int.* 34 (4), 362–377. <https://doi.org/10.3109/03093646.2010.520054>.
- Hobara, H., et al., 2020. Loading rates in unilateral transfemoral amputees with running-specific prostheses across a range of speeds. *Clin. Biomech.* 75, 104999. <https://doi.org/10.1016/j.clinbiomech.2020.104999>.
- Hoyt, B.W., Walsh, S.A., Forsberg, J.A., 2020. Osseointegrated prostheses for the rehabilitation of amputees (OPRA): results and clinical perspective. *Expert Rev Med Devices* 17 (1), 17–25. <https://doi.org/10.1080/17434440.2020.1704623>.
- Jarvis, H.L., et al., 2017. Temporal spatial and metabolic measures of walking in highly functional individuals with lower limb amputations. *Arch. Phys. Med. Rehabil.* 98 (7), 1389–1399. <https://doi.org/10.1016/j.apmr.2016.09.134>.
- Juhnke, D., et al., 2015. Fifteen years of experience with integral-leg-prosthesis: cohort study of artificial limb attachment system. *J. Rehabil. Res. Dev.* 52 (4), 407–420. <https://doi.org/10.1682/jrrd.2014.11.0280>.
- Kahle, J.T., Highsmith, M.J., Hubbard, S.L., 2008. Comparison of nonmicroprocessor knee mechanism versus C-leg on prosthesis evaluation questionnaire, stumbles, falls, walking tests, stair descent, and knee preference. *J. Rehabil. Res. Dev.* 45 (1), 1–14.
- Kannenberg, A., et al., 2013. Activities of daily living: genium bionic prosthetic knee compared with C-Leg. *JPO: J. Prosthet. Orthot.* 25 (3).
- Kaufman, K.R., Frittoli, S., Frigo, C.A., 2012. Gait asymmetry of transfemoral amputees using mechanical and microprocessor-controlled prosthetic knees. *Clin. Biomech.* 27 (5), 460–465. <https://doi.org/10.1016/j.clinbiomech.2011.11.011>.
- Kaufman, K.R., Bernhardt, K.A., Symms, K., 2018. Functional assessment and satisfaction of transfemoral amputees with low mobility (FASTK2): a clinical trial of microprocessor-controlled vs. non-microprocessor-controlled knees. *Clin. Biomech.* 58, 116–122. <https://doi.org/10.1016/j.clinbiomech.2018.07.012>.
- Kobayashi, T., Orendurff, M.S., Boone, D.A., 2013. Effect of alignment changes on socket reaction moments during gait in transfemoral and knee-disarticulation prostheses: case series. *J. Biomech.* 46 (14), 2539–2545. <https://doi.org/10.1016/j.jbiomech.2013.07.012>.
- Koehler, S.R., Dhaher, Y.Y., Hansen, A.H., 2014. Cross-validation of a portable, six-degree-of-freedom load cell for use in lower-limb prosthetics research. *J. Biomech.* 47 (6), 1542–1547. <https://doi.org/10.1016/j.jbiomech.2014.01.048>.
- Kunutsor, S.K., Gillatt, D., Blom, A.W., 2018. Systematic review of the safety and efficacy of osseointegration prosthesis after limb amputation. *Br. J. Surg.* 105 (13), 1731–1741. <https://doi.org/10.1002/bjs.11005>.
- Lee, W., et al., 2007. Evidence-Based Rehabilitation of Amputees Using Osseointegrated Prostheses: Applications of Finite Element Modelling in XIIth World Congress of the International Society of Prosthetics and Orthotics. Vancouver, Canada.
- Lee, W., et al., 2008b. Magnitude and variability of loading on the osseointegrated implant of transfemoral amputees during walking. *Med. Eng. Phys.* 30 (7), 825–833. <https://doi.org/10.1016/j.medengphy.2007.09.003>.
- Lee, W.C., et al., 2008a. FE stress analysis of the interface between the bone and an osseointegrated implant for amputees—implications to refine the rehabilitation program. *Clin Biomech (Bristol, Avon)* 23 (10), 1243–1250. <https://doi.org/10.1016/j.clinbiomech.2008.06.012>.
- Leijendekkers, R.A., et al., 2017. Comparison of bone-anchored prostheses and socket prostheses for patients with a lower extremity amputation: a systematic review. *Disabil. Rehabil.* 39 (11), 1045–1058. <https://doi.org/10.1080/09638288.2016.1186752>.
- Lura, D.J., et al., 2015. Differences in knee flexion between the Genium and C-leg microprocessor knees while walking on level ground and ramps. *Clin. Biomech.* 30 (2), 175–181. <https://doi.org/10.1016/j.clinbiomech.2014.12.003>.
- Meulenbelt, H.E., et al., 2006. Skin problems in lower limb amputees: a systematic review. *Disabil. Rehabil.* 28 (10), 603–608. <https://doi.org/10.1080/09638280500277032>.
- Morgenroth, D.C., 2013. Prescribing physician perspective on microprocessor-controlled prosthetic knees. *JPO J. Prosthet. Orthotics* 25 (4S), P53–P55. <https://doi.org/10.1097/JPO.0b013e3182a88d02>.
- Morgenroth, D.C., et al., 2018. Transfemoral amputee intact limb loading and compensatory gait mechanics during down slope ambulation and the effect of prosthetic knee mechanisms. *Clin. Biomech.* 55, 65–72. <https://doi.org/10.1016/j.clinbiomech.2018.04.007>.
- Newcombe, L., et al., 2013. Effect of amputation level on the stress transferred to the femur by an artificial limb directly attached to the bone. *Med. Eng. Phys.* 35 (12), 1744–1753. <https://doi.org/10.1016/j.medengphy.2013.07.007>.
- Niswander, W., Wang, W., Baumann, A.P., 2020. Characterizing loads at transfemoral osseointegrated implants. *Med. Eng. Phys.* 84, 103–114. <https://doi.org/10.1016/j.medengphy.2020.08.005>.
- OPRA, 2016. Implant System Instructions for Use. https://www.accessdata.fda.gov/cdrh_docs/pdf8/H080004D.pdf.
- Orendurff, M., et al., 2006. Gait efficiency using the C-leg. *J. Rehabil. Res. Dev.* 43 (2), 239–246.
- Pantall, A., Durham, S., Ewins, D., 2011. Surface electromyographic activity of five residual limb muscles recorded during isometric contraction in transfemoral amputees with osseointegrated prostheses. *Clin Biomech (Bristol, Avon)* 26 (7), 760–765. <https://doi.org/10.1016/j.clinbiomech.2011.03.008>.
- Pitkin, M., 2013. Design features of implants for direct skeletal attachment of limb prostheses. *J. Biomed. Mater. Res. A* 101 (11), 3339–3348. <https://doi.org/10.1002/jbm.a.34606>.
- Pitkin, M., Frossard, L., 2021. Loading effect of prosthetic Feet's anthropomorphicity on transtibial osseointegrated implant. *Mil. Med.* 186 (Suppl. 1), 681–687. <https://doi.org/10.1093/milmed/usaa461>.
- Prochor, P., Frossard, L., Sajewicz, E., 2020. Effect of the material's stiffness on stress-shielding in osseointegrated implants for bone-anchored prostheses: a numerical analysis and initial benchmark data. *Acta Bioeng. Biomech.* 2020 (2) <https://doi.org/10.37190/ABB-01543-2020-02>.
- Reid, S.M., et al., 2007. Knee biomechanics of alternate stair ambulation patterns. *Med. Sci. Sports Exerc.* 39 (11), 2005–2011. <https://doi.org/10.1249/mss.0b013e31814538c8>.
- Robinson, D.L., et al., 2020a. Load response of an osseointegrated implant used in the treatment of unilateral transfemoral amputation: an early implant loosening case study. *Clin Biomech (Bristol, Avon)* 73, 201–212. <https://doi.org/10.1016/j.clinbiomech.2020.01.017>.
- Robinson, D.L., et al., 2020b. Load response of an osseointegrated implant used in the treatment of unilateral transfemoral amputation: an early implant loosening case study. *Clin. Biomech.* 73, 201–212. <https://doi.org/10.1016/j.clinbiomech.2020.01.017>.
- Samuelsson, K.A., et al., 2012. Effects of lower limb prosthesis on activity, participation, and quality of life: a systematic review. *Prosthetics Orthot. Int.* 36 (2), 145–158. <https://doi.org/10.1177/0309364611432794>.
- Sawers, A.B., Hafner, B.J., 2013. Outcomes associated with the use of microprocessor-controlled prosthetic knees among individuals with unilateral transfemoral limb loss: a systematic review. *J. Rehabil. Res. Dev.* 50 (3), 273–314.
- Schmalz, T., Blumentritt, S., Jarasch, R., 2002. Energy expenditure and biomechanical characteristics of lower limb amputee gait: the influence of prosthetic alignment and different prosthetic components. *Gait Posture* 16 (3), 255–263.
- Schmalz, T., et al., 2014. Effects of adaptation to a functionally new prosthetic lower-limb component: results of biomechanical tests immediately after fitting and after 3 months of use. *JPO: J. Prosthet. Orthot.* 26 (3), 134–143. <https://doi.org/10.1097/jpo.0000000000000028>.
- Schwarze, M., et al., 2014. Influence of transfemoral amputation length on resulting loads at the osseointegrated prosthesis fixation during walking and falling. *Clin Biomech (Bristol, Avon)* 29 (3), 272–276. <https://doi.org/10.1016/j.clinbiomech.2013.11.023>.
- Stenlund, P., et al., 2017. Effect of load on the bone around bone-anchored amputation prostheses. *J. Orthop. Res.* 35 (5), 1113–1122. <https://doi.org/10.1002/jor.23352>.
- Stephenson, P., Seedhom, B.B., 2002. Estimation of forces at the interface between an artificial limb and an implant directly fixed into the femur in above-knee amputees. *J. Orthop. Sci.* 7 (3), 192–297.
- Struchkov, V., Buckley, J.G., 2016. Biomechanics of ramp descent in unilateral transtibial amputees: comparison of a microprocessor controlled foot with conventional ankle-foot mechanisms. *Clin. Biomech.* 32, 164–170. <https://doi.org/10.1016/j.clinbiomech.2015.11.015>.
- Thesleff, A., et al., 2018. Biomechanical characterisation of bone-anchored implant Systems for Amputation Limb Prostheses: a systematic review. *Ann. Biomed. Eng.* <https://doi.org/10.1007/s10439-017-1976-4>.
- van Eck, C.F., McGough, R.L., 2015. Clinical outcome of osseointegrated prostheses for lower extremity amputations: a systematic review of the literature. *Curr. Orthop. Practice* 26 (4), 349–357. <https://doi.org/10.1097/bco.0000000000000248>.